DOCUMENT

DELIVERABLE NUMBER	**D7.3**	DUE DATE	**30/11/2011**
ISSUED BY	**CRF**	ACTUAL DATE	**31/01/2012**
CONTRIBUTING WP/TASK	**WP7/ TASK 7.3**	PAGES	**31**
CONFIDENTIALITY STATUS	**PUBLIC**	ANNEXES	**-**

PROJECT

GRANT AGREEMENT NO.	**216049**
ACRONYM	**ADOSE**
TITLE	**RELIABLE APPLICATION SPECIFIC DETECTION OF ROAD USERS WITH VEHICLE ON-BOARD SENSORS**
CALL	**FP7-ICT-2007-1**
FUNDING SCHEME	**STREP**

DELIVERABLE D7.3
AUTOMOTIVE TESTS OF THE SENSOR MODULES

AUTHORS

CRF	**D. CAPELLO** **D. MORRA**
AIT	**C. SULZBACHNER**

APPROVAL

WORKPACKAGE LEADER	**CRF**	**D. CAPELLO**
PROJECT COORDINATOR	**CRF**	**N. PALLARO**

AUTHORISATION

PROJECT OFFICER	**EUROPEAN COMMISSION**	**I. HEIBER**

REVISION HISTORY				
VER.	**DATE**	**PAG.**	**NOTES**	**AUTHOR**
01	20/01/2012	All	Initial version	D. Capello (CRF)
02	24/01/2012		SRS description FIR-NIR description	C. Sulzbachner (AIT) G. Monchiero (MM) D. Fontana (MM)
03	31/01/2012		MFOS sensor	D. Morra, D. Capello (CRF)

TABLE OF CONTENTS

1. INTRODUCTION

This report summarises the tests performed with the developed sensors (MFOS, FIR and SRS), installed on two vehicle demonstrators, one from CRF and another one from AIT. For each sensor the methodology and test plan description, the analysis of results and the conclusions have been provided.

2. MFOS SENSOR

The functional tests of the MFOS sensor described in this section refer to the environmental detection functionalities. Active night vision function is described in chapter 3 with FIR sensor for enhanced night vision application. The MFOS sensor is based on a dioptric lightguide and allows the detection of fog and twilight by two dedicated ROIs in the imager corners and rain and tunnel using the frontal monitoring area.

2.1 Twilight/tunnel function

2.1.1 Methodology and test plan description

The twilight function is assessed proving the correct activation of low beams (in ADOSE project it is a virtual actuation) as soon as the environmental illumination drops below a threshold value that in most cases, as described in D7.1, ranges between 500 to 1500 Lux. Several tests are needed to prove the correct activation also in dynamic conditions and in complex illuminated scenarios with tree and building shadows, etc. Moreover, the robustness of the algorithms needs to be verified also in cases that could generate false alarms such as for instance artificial illuminated streets.
The twilight function is also matched with the tunnel detection function. The general performances of this function are evaluated in real conditions verifying the activation of the low beams while the equipped vehicle is approaching the tunnel entrance and the switching off as soon as the vehicle has left the tunnel. Trials need to be performed even to prove that not false detections are counted, i.e. by discriminating the presence of a bridge or a tunnel.
During the project, a total of about 250 tests have been performed. Some tunnel detection has been evaluated more than one time per tunnel in both directions. Trials have been focalised in daylight clear and cloudy conditions, and in urban and extra-urban scenarios.
The following picture summarises the sites in which the tunnel detection has been tested. Sites A, B are tunnel along highways (two lines per direction), site E is an extra-urban tunnel with two lines per direction, site C is an extra-urban tunnel with one line per direction. D sites puts together some urban tunnels. Bridges have been encountered most of all in highways and extra-urban roads (A, B and E sites).

Figure 1 - Twilight / tunnel test sites

Figure 2 - Two consecutive tunnels in the E site

2.1.2 Analysis of the results

The following table summarizes the trials conditions and the results for the twilight/tunnel function. The first two columns report the environmental condition and the scenario in which the trials have been carried out. The target column highlights which function/evaluation parameter has been tested. In the case of twilight function, the activation of low beams below a predefined illuminance needs to be verified as well as the detection/recognition of tunnels - for low beams early activation - or bridges, for which no action should be taken. The errors column shows the respective error respect to the ground-truth. Error results could be missed detection or activations. In the bridge and tunnel targets, some trials were devoted to count the false detections, even if, in the considered tests, no false have been seen.

Environmental condition	Scenario	Target	Trials	Errors
daylight, clear	urban	twilight	20	0
		bridge	8	0
		tunnel	15	0
daylight, clear	extraurban	bridge	47	0
		tunnel	34	2
daylight, cloudy	urban	twilight	35	4
		bridge	4	0
		tunnel	15	0
daylight, cloudy	extraurban	bridge	46	0
		tunnel	28	2

Table 1 - Results of twilight / Tunnel function

The above mentioned results can be summarized as follows:

- Tunnel entrance: detection in almost all analyzed cases. Some missed detections (limited early activation) due to VFOV.
- Tunnel exit: actuation affected by illuminance values. Slower at values near twilight threshold.
- Bridges: 100% detection in all conditions.
- Tunnels and bridges: no false detections for the considered trials.
- Twilight: actuation in almost all conditions. Some wrong (early) actuation in urban scenarios (avenues with trees), in twilight conditions.

2.1.3 Conclusions

Twilight and tunnel functions performances have been assessed in many conditions, some of which critical and suitable to stress the function behaviour. Although quantified evaluation and comparison (with SOA sensors) thresholds have not been a-priori defined, the MFOS sensor proved to satisfy common functional requirements that could be verified by trained customers.

2.2 Fog function

2.2.1 Methodology and test plan description

After the static characterization tests carried out in real condition using vapor spray and described in D7.1, fog function has been evaluated in real scenarios in urban, extra-urban and highway during foggy and clear days in daytime and nighttime conditions. The first two scenarios allow to evaluate how the function behavior is affected by the vehicle relative speed respect to the fog particles. The latter two allow to verify if the IR emitter output radiation is well designed to cover the dynamic range in real conditions. Moreover, some trials have been also carried out during clear days in order to check for false detections.
A total of about 100 trials have been made in the near-by of Turin as can be seen in the following picture showing the trial ways.

Figure 3 - Fog test sites

Figure 4 - Fog clearing during a trial in the B site

2.2.2 Analysis of the results

Fog activation and detection, as explained in WP3 and D7.1 deliverables, is based on the amount of backscattered radiation that is collected and focalised in the dedicated corner ROI in the CMOS imager. For this scope, the imager response is set linear and the computation of the ROI mean digital values is done using two frames, the first one when the IR emitter is switched on and the second one when it is switched off. The virtual actuation of the fog beams is performed when the calculated difference is above a threshold that has been defined during tests in 7.1 task. In ADOSE project, a value of 30 has been set. In order to prevent accidentally activations, a median filter is figured out and an hysteresis cycle allows to avoid blinking due to values near the threshold. In the following figure, the acquisition data of about 7 minutes taken in the ringroad labelled G in mixed foggy-clear conditions is shown. The purple solid line are the computed frame differences taken each time the trigger pulses the IR emitter (about every 2 seconds). The blue line are the filtered data that are compared to the orange threshold value to determine the activation conditions.

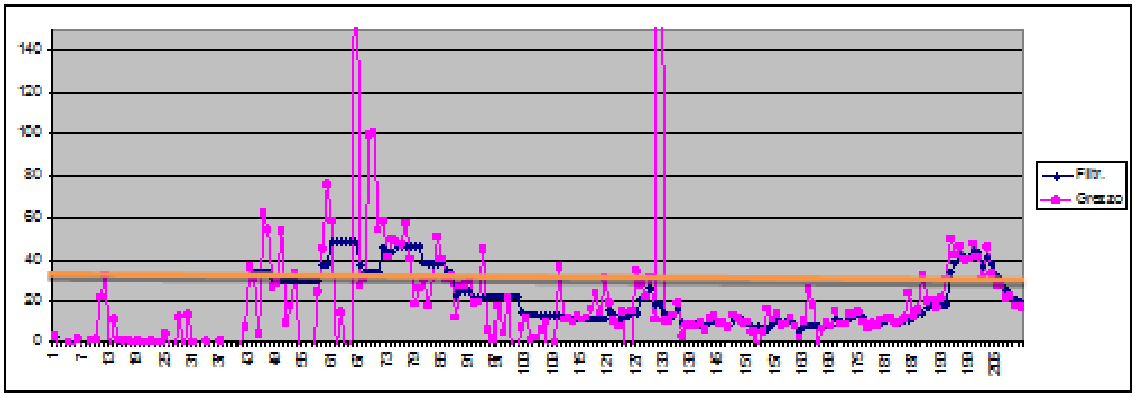

Figure 5 - Data acquired during a test campaign in the ringroad

The following table is the summary of the results taken in the conditions described in the aforementioned paragraph. For each site, depending on the stability of the environmental condition, several trials have been carried out. The column error has to be interpreted as missed detection in case of the presence of fog (see environmental condition column) or as false alarm in case of a clear condition.

Environmental condition	Scenario	Trials	Errors
daytime, clear	urban	13	0
	extraurban	9	0
	highway	4	0
daytime, foggy	urban	15	1
	extraurban	15	4
	highway	9	3
nightime, clear	urban	8	0
	extraurban	6	0
	highway	4	0

nightime, foggy	urban	11	0
	extraurban	10	2
	highway	3	0

Table 2 - Results of fog function

Results show that no false alarm have been registered during the runned trials both in daylight and in nighttime conditions. Some missed detections have been seen in highway and extra-urban scenarios caused by the vehicle speed which badly affects the backscattered radiation in non-homogeneous particle density. Although the not high number of trials, which prevents to take statistically consistent considerations, we can see that missed detection are most probably during daytime respect to nightime conditions. This consideration is validated also taking into account the missed detections. In fact, some errors are present during daytime in all scenarios. The reason could be explained considering the high background illumination level that limits the function dynamic range. This limitation, as explained in D7.1, rises from the design of the IR illuminator that favored the low cost and easy to assembly requirements taking standard off-the-shelf infrared LEDs and plastic collimating optics. Using a dedicated infrared emitter (that could be designed and easily molded reaching at the same the low cost goal) and optics the overlapping cones formed by the optics FOV and LED emitting angle could be further optimized.

2.2.3 Conclusions

The assessment of the fog function has been done in different scenarios and illumination conditions. Although the number of trials seems not to be particularly high, the considered conditions under which the trials have been performed allow to reach some conclusions. Fog function performances in terms of missed detections are affected by vehicle speed, particularly in not-homogeneous fog particle density conditions, and by high environmental illumination levels which limit the functional dynamic range due to the combination of the emitting infrared output of the illuminator and the FOV. In particular the latter limitation could be overcome by adopting dedicated collimating optics. Furthermore, no false positive errors have been observed.

2.3 Rain function

2.3.1 Methodology and test plan description

The rain function has been characterized in real scenarios, urban and extra-urban, in daytime and nightime conditions. The current development of the function, as explained in D7.1, did not allow a complete and exhaustive validation, nevertheless about 65 trials were done under light and heavy rain environmental conditions.
The following picture shows the test sites made in the near-by of Turin.

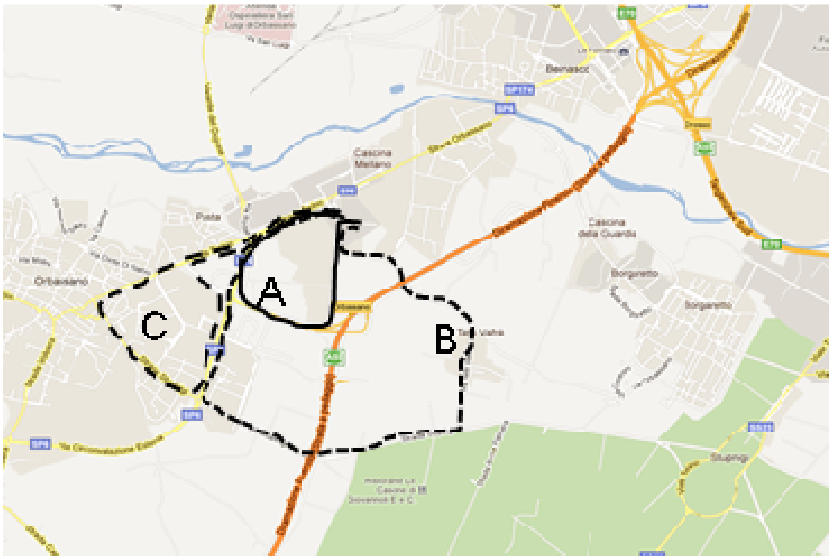

Figure 6 - Rain function test sites

Figure 7 - On-the-vehicle image taken during a trial in CRF

2.3.2 Analysis of the results

The following table summarizes the trials conditions and the results of the rain function validation. As for the previous described functions, the columns report the environmental conditions and scenarios under which tests have been carried out, the number of trials and the number of missed detections and false alarms.

Environmental condition	Scenario	Trials	Missed detections	False alarm
daylight, light rain	city, generic and trees	10	2	4
	Extraurban	14	2	5
daylight, heavy rain	city, generic and trees	12	1	3
	Extraurban	15	3	3
nightime	city, generic	8	1	1
	Extraurban	6	2	0

Table 3 - Results of rain function

Approximately 15% of missed detections have been counted due to a couple of reasons:

- speed causes droplets to be slipped thus changing the curvature respect to stationary condition;
- as observed in the characterisation phase, limited FOV lead to only few droplets to be in the right position to be detected.

Finally, a sensible amount of false alarms could have been observed. In this case the limitation of the Matlab code developed in the ADOSE SW framework brought to the impossibility to analyse consecutive frames with IRLED switched on and off. At the end this consideration, in conjunction to the speed which causes background variability, had raised the false positive to about 20%.

2.3.3 Conclusions

Despite the not fully integration of the rain function in the ADOSE SW framework, a validation and assessment of the functionality performances have been carried out not only in stationary conditions but also in real outdoor scenarios. The selected approach for the detection of the rain droplets is promising and performances could be further improved adopting design strategies aiming at overcoming the identified limitations.

3. FIR SENSOR

3.1 Enhanced night vision (FIR/NIR) function

Enhanced night vision functionality is addressed by combining FIR low resolution sensor and the MFOS NIR camera through pre-processing and application-oriented algorithms.
The FIR camera that has been used for the trial campaign is the first developed prototype by BOSCH characterized by low resolution (42x28 px) respect to the target spec of 100x50 px, higher NETD, low frame rate (about 5Hz considering the thermal time constant respect to the target 25Hz) and a preliminary plastic camera package. As expected, all these limitations badly affects the function performances. The final FIR prototype version satisfying most of all ADOSE specs has been made available by the end of the project and it was showed, installed on CRF's vehicle prototype, for the final demonstration. Some of the qualitative results have been reported at the end of section 3.1.2.

3.1.1 Methodology and test plan description

This section describes the HW and SW tools that have been implemented and used in order to perform the enhanced night vision functional tests. Furthermore, a description of the methodology is provided.

Regarding the HW and SW, the following tools were considered.

Hardware:

- FIR camera
- MFOS NIR sensor
- FLIR camera (commercial FIR)
- Laser radar

The FLIR camera has been installed on the ADOSE vehicle prototype and has been used for the comparison of the acquired FIR scenes. The ADOSE vehicle has also been equipped with a laser radar with the goal to perform distance measurements in dynamic conditions (Figure 8).

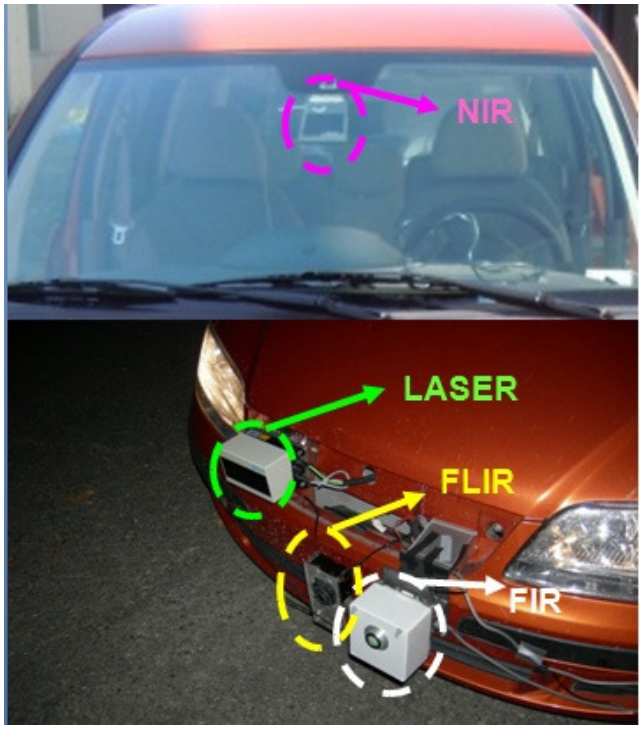

Figure 8 - ADOSE demo prototypes during installation

Software:

- ADOSE Framework
- Laser Testing
- FIR Video Converter
- PGM Video Player v 3.0

The ADOSE framework displays the acquired images through a GUI and performs the obstacle detection.

Then an analyzer tool for test and characterization of LIDAR data, synchronous with the MFOS NIR sensor, has been developed. The SW allows the handling of laser data and information exchange with the ADOSE framework.

Since each sensor has different format resolutions (Table 4), a SW tool with the goal to handle FLIR data modifying (rescaling and sub-sampling the format, resolution (42x28) and frame rate (12fps)) has been developed.
Moreover the FIR video converter allows the conversion of the video bitstream stored in an AVI file into a sequence of image files compatible with the ADOSE framework and compliant with the Bosch camera resolution.
The video input is a B&W video bitstream with a resolution of 720x540 pixels de-interlaced, with a pixel resolution of 8bit for pixel (0 for cold pixel, 255 for hot pixel).

Sensors	Pixel Resolution
FIR (low cost FIR)	42 x 28
FLIR (commercial FIR)	320 x 240
MFOS NIR	1024 x 512

Table 4 - List of cameras and their format resolutions

As could be seen in the following figure, the video handling chain is at first digitalized in an MPEG file (full resolution) by means of a video grabber and then a preliminary conversion in an AVI uncompressed format is performed.

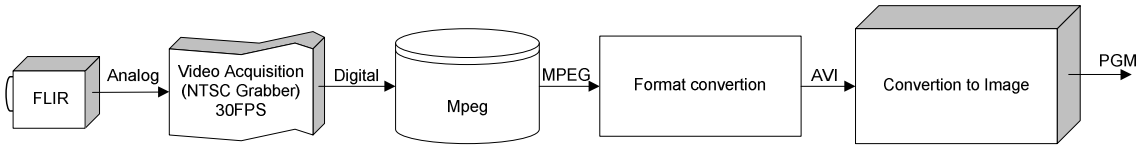

Figure 9 - Video handling chain of the FLIR camera

The following figure shows one screenshot of the FIR video converter program. On the left the original video is displayed while on the right the rescaled one. It is also possible to select the resolution and the output framerate.

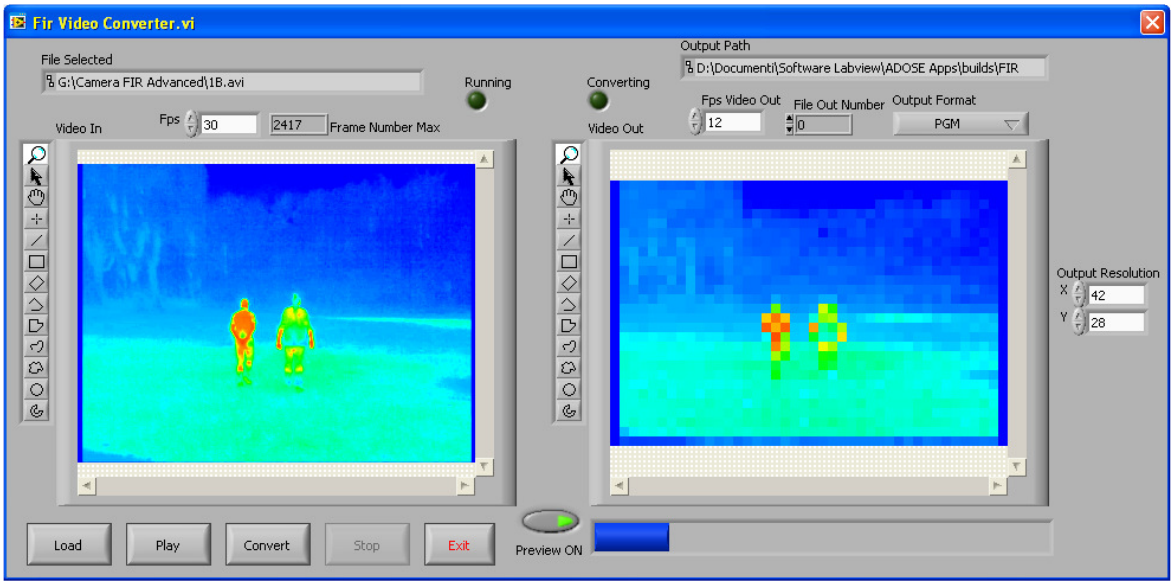

Figure 10 - FIR Video Converter GUI

Finally, the PGM Video Player 3.0 SW tool has been developed in order to evaluate the system performances. This program allows to change the thresholds and select the frame rate in order to easily read the max and min values of a video file. Moreover, by setting the NIR/FIR parameters - namely the FOV, the size of image (H,W), the positions of the two sensors (X,Y,Z)

and the pitch, yaw and roll angles of the sensors - it also allows to detect blobs on the FIR image.

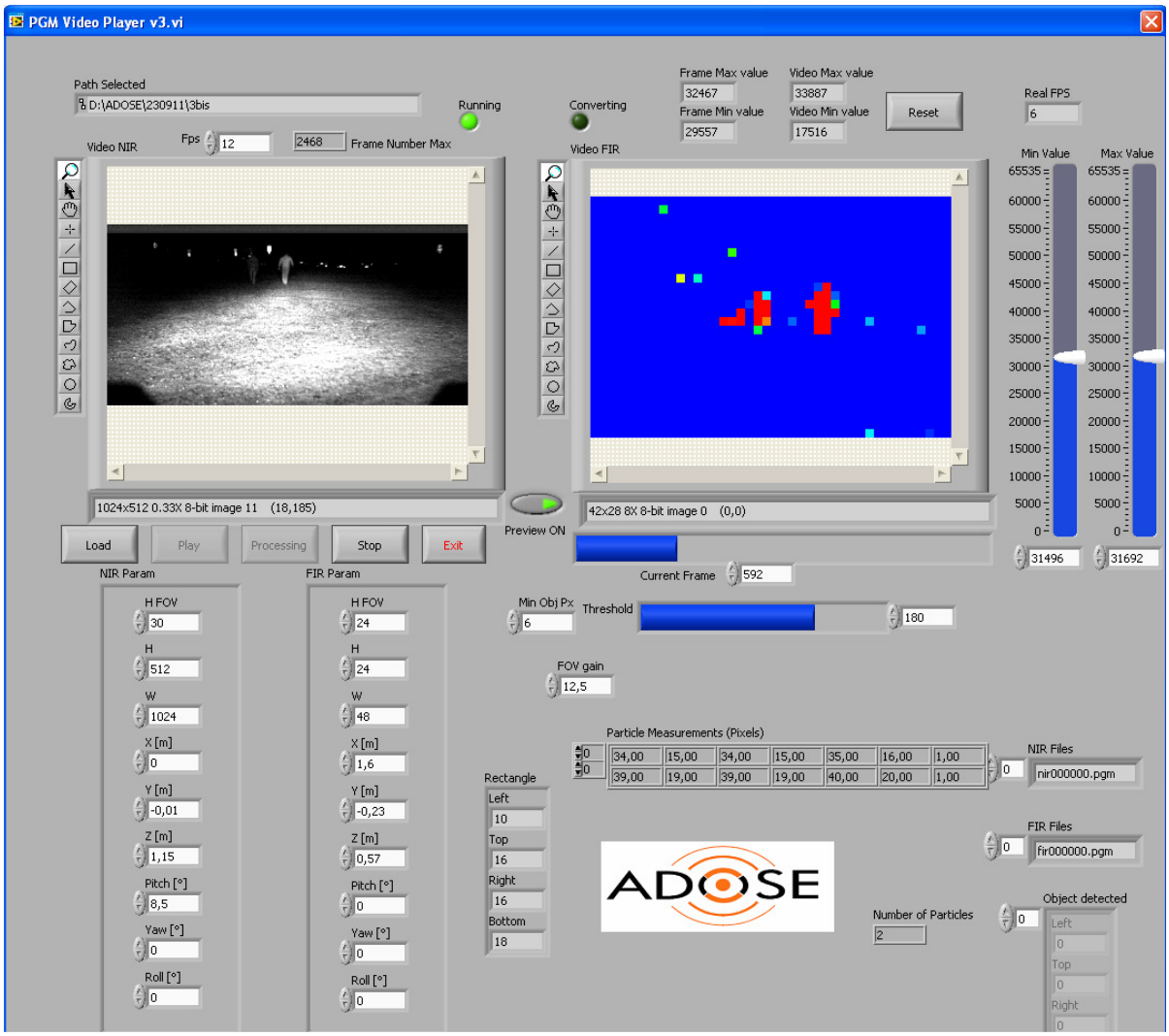

Figure 11 - PGM Video Player 3.0 GUI

Regarding the methodology, functional static tests in controlled outdoor conditions have been done to determine the performance baseline of the function. These tests have also been used to select the most appropriate camera settings. Then a test plan in order to investigate sensor behaviours in real environment and dynamic conditions was set up. The test plan includes:

- vehicles and pedestrians
- different sizes and shapes
- different direction of vehicle target
- different illumination conditions
- target in movement
- tests in urban area

3.1.2 Analysis of the results

Static outdoor tests in controlled conditions have been carried out in order to figure out the maximum detection distances in ideal conditions. The trials have been done using vehicles, pedestrians (ecto and endo-morphic), etc.
The targets have been placed at different distances and measurements have been repeated in order provide statistically consistent outputs; at each step the targets have been moved away of about 5m from the sensor. The output results are collected in the following tables:

	Nr. Of Test with a Car	Detected from 25 m	Detected from 30 m	Detected from 35 m	Detected from 40 m	Detected from 45 m	Detected from 50 m	Detected from 55 m	Detected from 60 m
Pedestrian A (normal body size)	10	10	9	6	4	1	0	0	0
Pedestrian B (stocky build)	10	10	10	10	8	5	4	3	3

Detection of the back side car	Nr. Of Test with a Car	Detected from 25 m	Detected from 30 m	Detected from 35 m	Detected from 40 m	Detected from 45 m	Detected from 50 m	Detected from 55 m	Detected from 60 m	Detected from 65 m	Detected from 70 m
Fiat Grande Punto	5	5	5	5	4	3	2	1	1	0	0
Alfa Romeo MiTo	5	5	5	4	4	3	1	1	0	0	0
Wolkswagen Golf	5	5	5	5	4	4	2	2	1	0	0

Detection of the front side car	Nr. Of Test with a Car	Detected from 25 m	Detected from 30 m	Detected from 35 m	Detected from 40 m	Detected from 45 m	Detected from 50 m	Detected from 55 m	Detected from 60 m	Detected from 65 m	Detected from 70 m
Fiat Grande Punto	5	5	5	5	5	4	3	3	2	1	1
Alfa Romeo MiTo	5	5	5	5	4	4	3	2	2	0	0
Wolkswagen Golf	5	5	5	5	5	5	4	3	2	1	1

Table 5 - Detection distances of pedestrians and vehicles in static outdoor conditions

The detection distances are all well below the target specs. As explained in the introduction, some characteristics of the tested BOSCH camera prototype – i.e. camera resolution and NETD above all, even in static conditions did not allow to reach the ADOSE goals.

Some examples of acquisitions to prove the above mentioned spec limitations are hereafter reported.
In the following example two pedestrians in open field are standing 35m away from the ADOSE vehicle. The images have been taken with the low beams switched ON and the IR illuminators switched OFF. The outside temperature was about 11 °C. On the left it is shown a screenshot of the ADOSE framework. In the upper part it could be seen the MFOS NIR image and in the lower one the FIR image. Due to the lack of illumination provided by the IR beams, the two pedestrians could not be easily recognized by the MFOS NIR sensor. The FIR image highlights some hot pixels that allow the detection of the two pedestrians which could be seen with the two blobs superimposed on the MFOS NIR image. It is evident the not sufficient resolution of the FIR image in order to distinguish the two pedestrians as two separate blobs. This conclusion could be also demonstrated looking in the right side of the image in which in the upper part the full resolution FLIR image is reported and in the lower one the rescaled FLIR image.

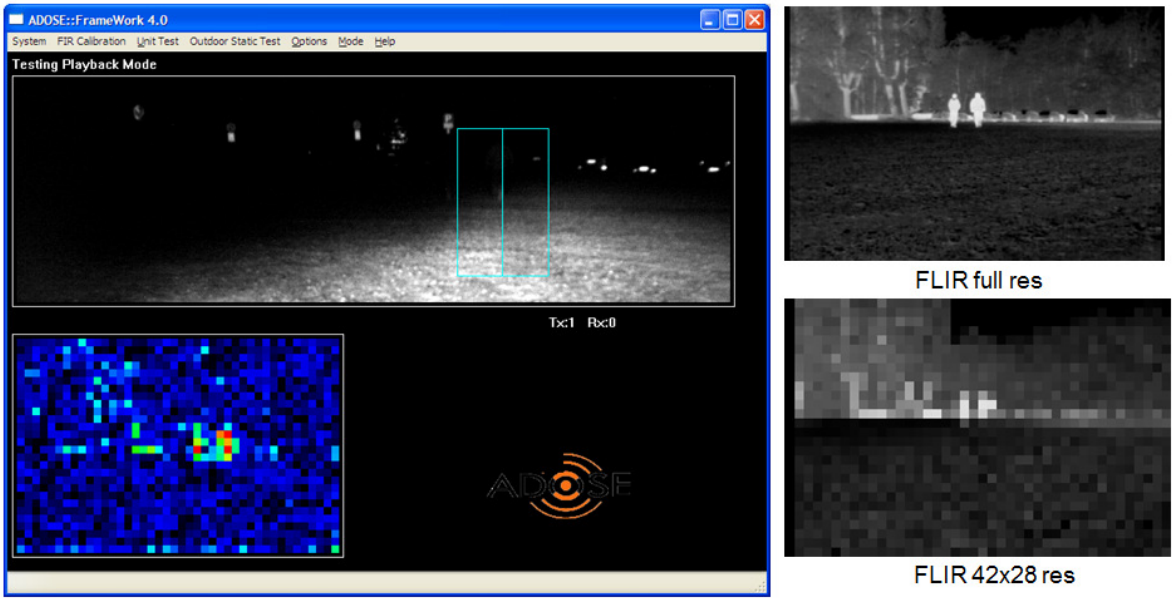

Figure 12 - Pedestrians standing at 35m distance

In this second example, in open field the vehicle equipped with FIR, FLIR and MFOS NIR sensors starts moving. At 30m distance a pedestrian and another vehicle are standing. Also in this case the IR illuminators are switched off so that the MFOS NIR image could not easily detects the pedestrian on the right part of the image. In the lower part of the ADOSE framework the FIR image provides hot and well contrasted pixels of the warmer area of the vehicle and of the pedestrian. The detection is possible even if the pedestrian and the vehicle subtend only few pixels narrowly aligned horizontally and vertically respectively. This means that the detection is only possible due to the high temperature contrast between hot and cold regions as could be also seen looking at the FLIR images.

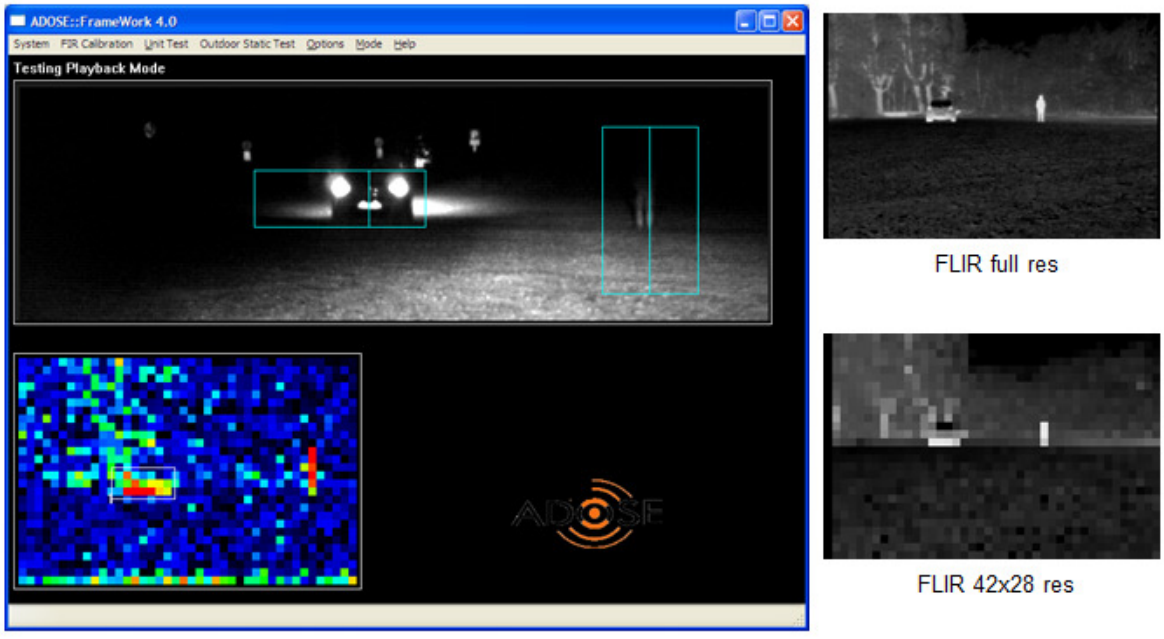

Figure 13 - Vehicle and pedestrian detection at 30m distance

The following test describes the vehicle equipped with FIR, FLIR and MFOS NIR sensors while it is approaching a vehicle standing in the right side of a straight road at 60m distance and immediately behind it a pedestrian is standing. Outside temperature was about 12 ℃ and the low and IR beams of the ego vehicle were turned on. In this case, the lack of resolution does not allow the pedestrian detection as could be observed by the rescaled FLIR image. Furthermore, high thermal noise could be seen in the FIR image which affects the overall image quality.

Figure 14 - Vehicle and pedestrian at 60m distance

This behaviour is even more evident in the following trial in which the ego vehicle is passing a pedestrian at 25m. The outside temperature is the same as the above described test. In this case the thermal noise and the high NETD could not provide useful contrast between the road and the pedestrian.

Figure 15 - Pedestrian standing at 25m distance

As far as the final camera prototype has being made available for tests during the ADOSE final meeting and demonstration session, some trials have been carried out in order to qualitative check the FIR camera performances comparing the final achievements with the results obtained with the first camera prototype.
For this reason, a condensed list of scenarios have been selected and are reported in the following table.

1 person approaching ego-car track from side, ego-car turning away from person
Ego-car approaching 2 persons (1 standing, 1 walking towards ego-car)
Ego-car approaching other car front to front
Ego-car approaching other car front to front and 1 person standing on other side of road
Ego-car stopped and facing group of persons

Table 6 - Test case for the existing ADOSE prototype on-vehicle

Trials results are reported in the following figure in which left images are with native resolution of the imager (100x50px), whereas the right ones have been modified with 3 times bicubic interpolation.

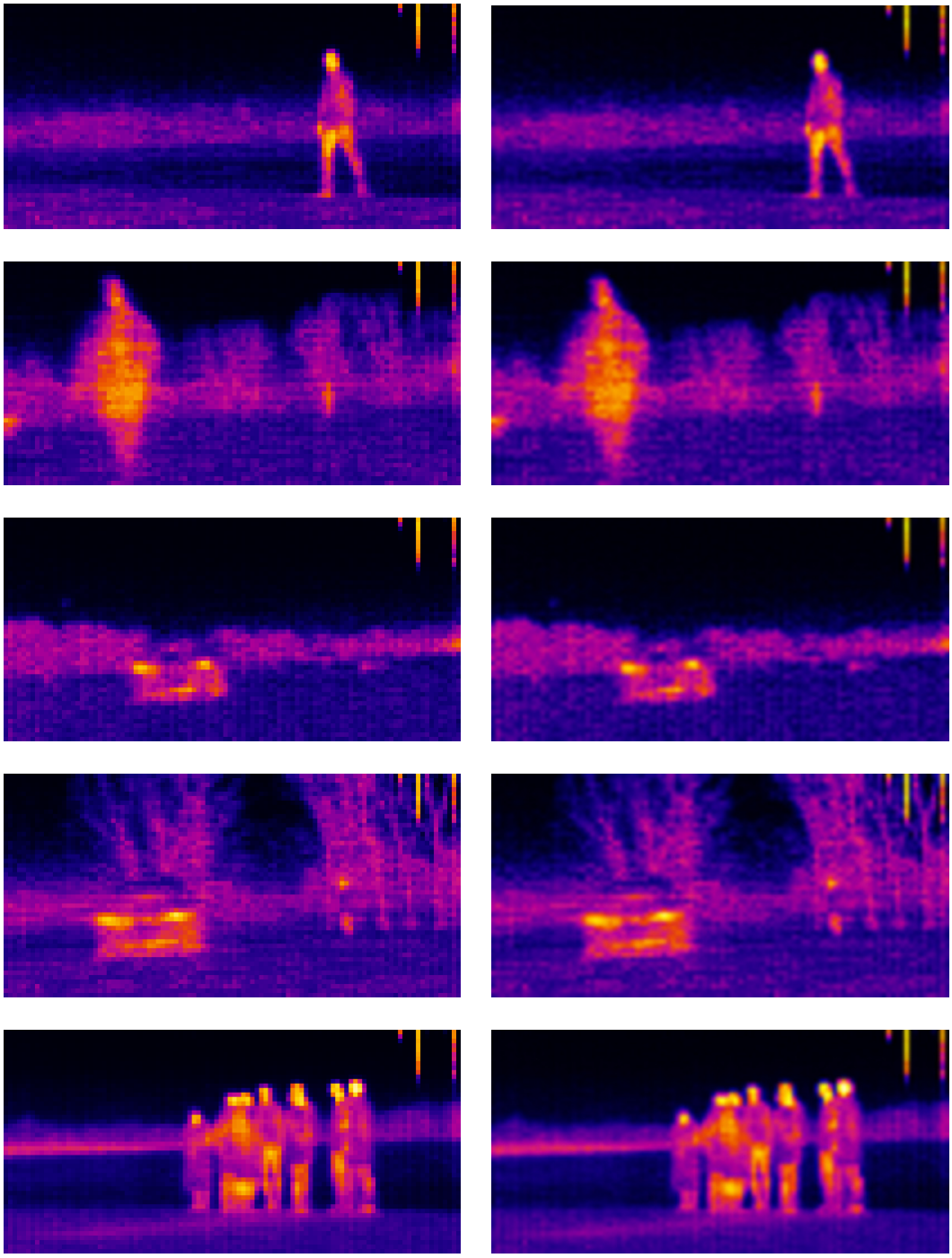

Figure 16 - Sample images from test cases taken with the final FIR camera prototype

As could be observed, the overall image qualities are better respect to the ones obtained with the first camera prototype. It could be seen that the increased image resolution and the low thermal noise allow to clearly recognize the obstacles. The good image contrast is also due to the low environmental temperature during the demo session of some degrees Celsius. Furthermore, for human recognition, in some images the bicubic interpolation helps in better recognizing the objects since it is reached the better trade-off between resolution and contrast.

Finally, some tests have been carried out by grabbing two pedestrians at increasing distances in order to qualitative estimate the detection distance. Measurements have been taken with acquisition steps of 4.7m using references already positioned at the Centro Sicurezza test track.
During this trial session, the environmental temperature was some degree Celsius above zero and the ADOSE vehicle has been positioned in the middle of the lane. Before the acquisition, the camera thermal calibration has been done.
As could be seen in the following images, the overall image noise is good. The high (around 30 ℃) temperature differences between the targets and the background allow to clearly recognize the hot objects. The imager resolution of the camera allows to identify the human silhouettes up to 40-50m distance. Then hot pixels are visible but obstacles are hardly identifiable without the a-priori knowledge of the pedestrian positions.

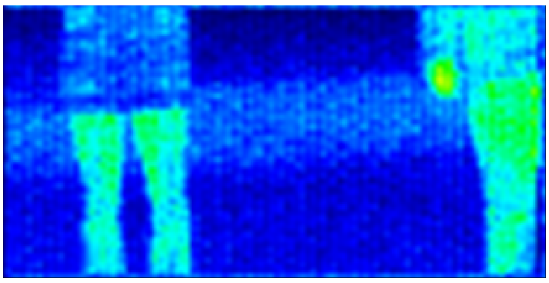
dist: 4.7m

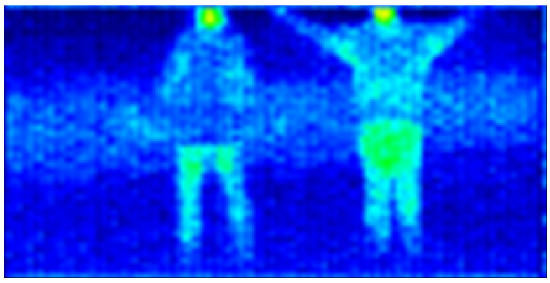
dist: 9.4m

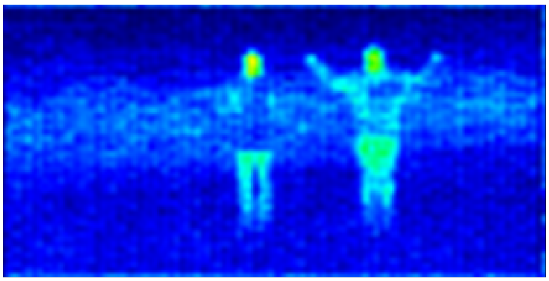
dist: 14.1m

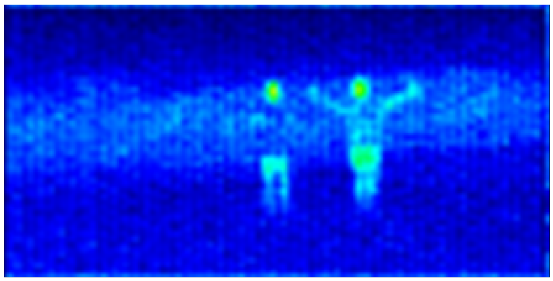
dist: 18.8m

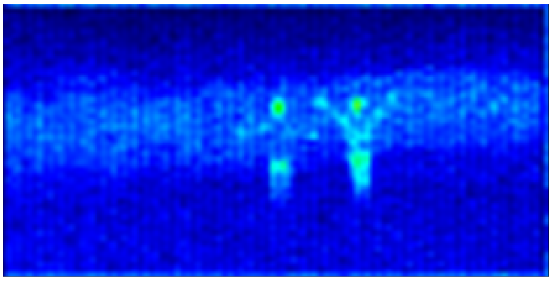
dist: 23.5m

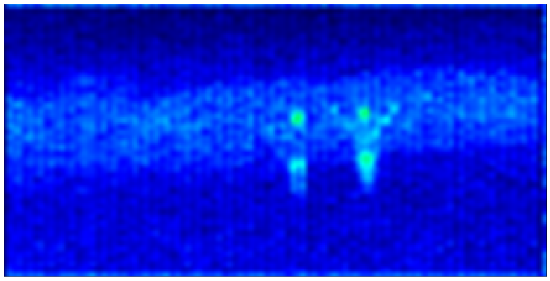
dist: 28.2m

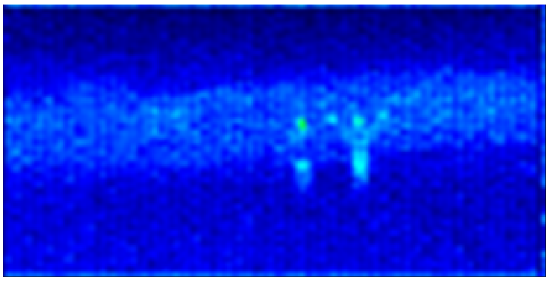
dist: 32.9m

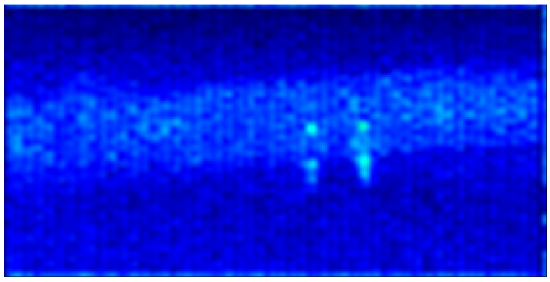
dist: 37.6m

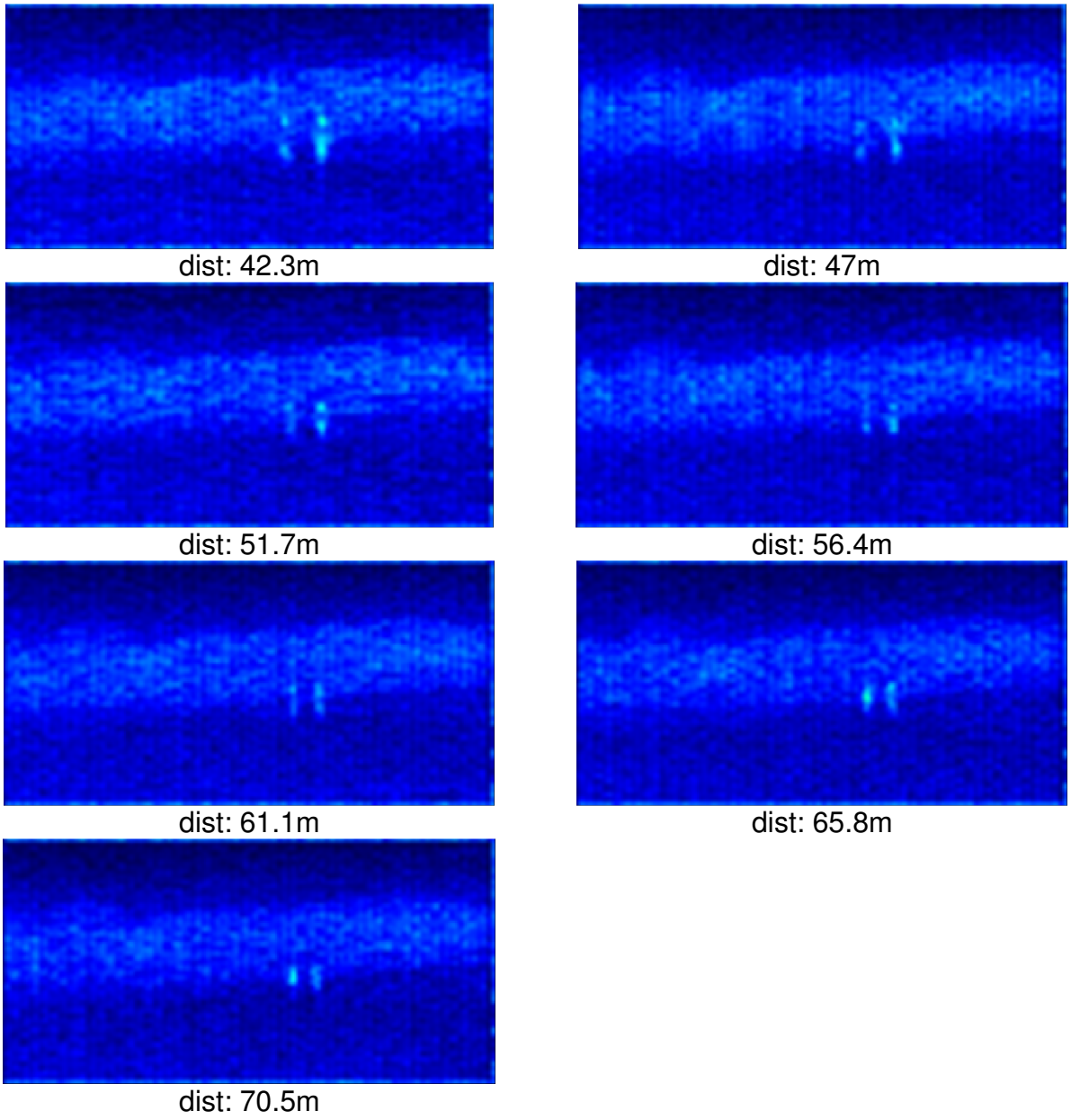

Figure 17 - Pedestrians standing at increasing distances from the ADOSE vehicle equipped with the final FIR camera prototype

3.1.3 Conclusions

The limited camera specs affected the overall detection performances. By the comparison of the images provided by a commercial FLIR camera rescaled to the resolution of the FIR one it could be figured out that the low resolution (~10°/px horizontal) impacts, as expected, the detection distance. Furthermore, the high thermal noise and the NETD, despite the fact that the tests have been carried out with outside temperature of about 12 °C, degrade the image qualities and the contrast between warm and cold objects. This behavior is also caused by the camera package in its preliminary version. More in details it could be said that the detection is not affected by

different car types and the human shape has an high impact (+25%). The maximum detection distances was 60m for a vehicle and 35m for a pedestrian. The low camera frame rate (around 5Hz) did not allowed to detect any obstacle with vehicle speed of more than 20km/h and target vehicle speed of more than 10km/h.
Last trials carried out using the final FIR camera version during the ADOSE final demo session demonstrated the potential benefits of the low cost and low resolution FIR camera technology. Even if not all the target specs have been reached the 100x50 px camera resolution together with the low thermal noise showed the possibility to clearly identify pedestrian obstacles up to 50m distance and hot pixels blobs up to 70m.

4. SRS SENSOR

4.1 Pre-crash side impact function

The SRS sensor has been further developed and enhanced to achieve the requirements of the side impact scenario. The detection range d for pre-crash warning/preparation must be greater than the distance a dangerous object could travel during the system reaction time of the countermeasure. This time consists of the overall response time of the sensor and reaction/decision time of the ADAS including activation time of the countermeasure (e.g. preparation of safety belts).
The requirements (see D1.2) stated that the assumed velocity of an approaching vehicle is of 60km/h, the minimum width w_{min} of the object is 0.5m, the detection area of the FOV is 30°, the detection distance d_{max} is 6m and the critical distance d_{min} is 5m as shown in the figure here below.

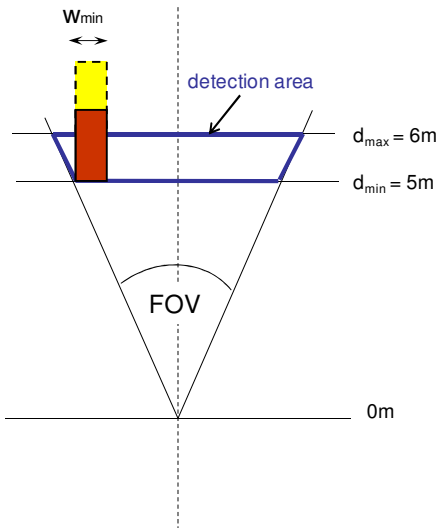

Figure 18 - SRS sensor detection range requirements

For practical issues the final stereo configuration was modified to a baseline of 0,15m with optics of a focal length of 12mm. Thus, the critical distance is equal to 12px disparity.

For performance reasons, the algorithm is configured to compute a disparity range of 20px starting from 0.

4.1.1 Methodology and test plan description

The test arrangement consists of the SRS sensor that is mounted at the side of the vehicle and a light barrier that is positioned at the critical distance of 5m that is equates to a time frame of 300ms before a possible collision. For details on the sensor integration into the vehicle see D7.2. For safety reasons during the tests the approaching vehicle drives through the FOV of the stereo sensor and crosses the detection area, without a collision. After passing the critical distance, the direction of the approaching vehicle is changed to avoid the standing vehicle.

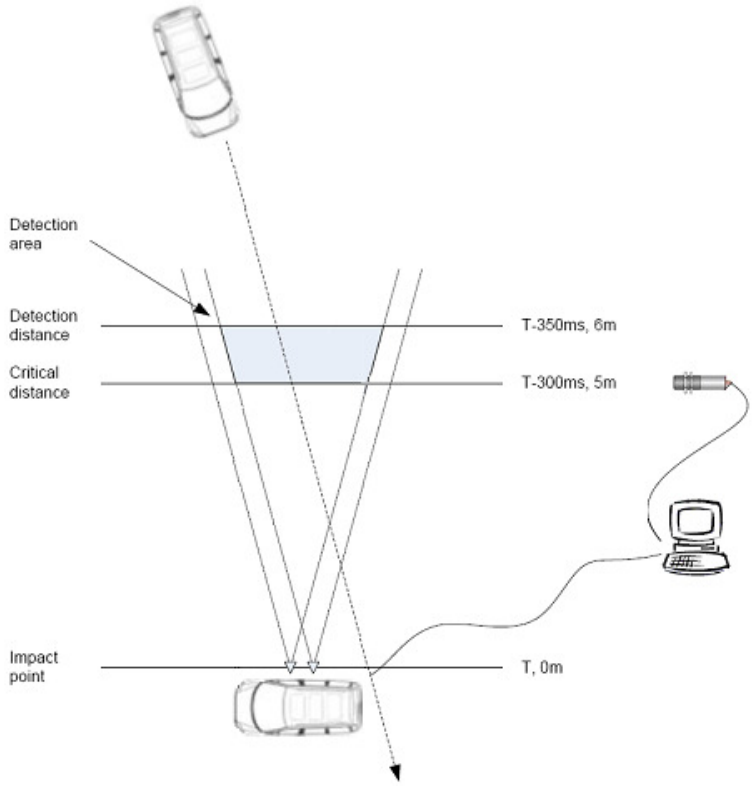

Figure 19 - Test setup for SRS sensor

Figure 19 shows the test setup of the driving scenarios. The test set include 10 driving scenarios where the following measurements were evaluated:

- Detection of the performance of the stereo vision and detection algorithm to indicate whether an approaching object is detected or not.
- Evaluate the absolute distance when the front bumper of the vehicle crosses a light barrier.

4.1.2 Analysis of the results

The performance criteria are to detect an approaching object before it is crossing the detection distance. In case of a positive detection, the respective object is framed with a bounding box.

When the approaching vehicle is crossing the light barrier the processing results will get frozen for later evaluation. The user is able to see if the approaching vehicle was detected or not. Table 7 shows the distances of the scenarios where an object was detected.

Scenario	Object Detected before critical distance
1	yes
2	yes
3	yes
4	yes
5	yes
6	yes
7	yes
8	yes
9	yes
10	yes

Table 7 - Evaluation of performance of SRS sensor

For measuring the absolute distances the same mechanism as mentioned before is used. When the vehicle is passing the critical distance the light barrier is generating a trigger used for the evaluation of the distance. The vehicle passes the light barrier with the bumper of the vehicle first and therefore, the distance of the bumper is used for the measurement of the current distance. Thus, the median disparity of the bumper is used for the comparison with critical distance. The standard deviation of the distance of detectable objects is 0.52 m in relation to an expectancy value of the critical distance.

Scenario	Object Detected		Offset to required detection distance
	avg. Disparity [px]	Distance [m]	[m]
1	11	5,45	0,45
2	14	4,61	0,39
3	13	4,29	0,71
4	13	4,29	0,71
5	15	4	1
6	14	4,61	0,39
7	13	4,29	0,71
8	14	4,61	0,39
9	15	4	1
10	15	4	1

Table 8 - Evaluation of performance of SRS sensor

4.1.3 Conclusions

The performance achieved by the final algorithm gives a standard deviation of the distance of a detectable object of 0.52m in relation to the required 5m critical distance.

With the results achieved by the sensor prototype assessed in real scenario, we conclude that the SRS together with its stereo matching and detection algorithms developed in this project are capable to meet the requirements even with the short baseline of 15 cm (45 cm of the first laboratory prototype).

The intention of the SRS to address the Automotive the Pre-Crash Warning/Preparation Side Impact, the Smart Airbags and the Lane change detection applications is proved to be valid.

In the long term, the SRS with its relatively low cost and fast response time has the potential to add value to the automotive market

5. FINAL DEMONSTRATION

5.1 Description

A demonstration event took place during the ADOSE final review meeting in the Centro Sicurezza test track near CRF premisis. The demo involved the FIAT Idea CRF's vehicle equipped with the MFOS sensor and the FIR camera and the FORD Focus AIT's vehicle equipped with the SRS sensor.

Figure 20 - FIAT Centro Sicurezza test track

Figure 21 - An highlight of the demonstration vehicles during the preparation

During the demonstration, it has been shown the precrash-side impact scenario usign both stationary and moving obstacles. Then, the equipments and the installaed sensors have been

presented and a demo of the MFOS environmental sensor functionalities (fog, rain detections) have been done. Finally, the demonstration of the warning night vision scenario involving several pedestrians and one approaching vehicle has been carried out.

Figure 22 - Pre-crash side impact demo

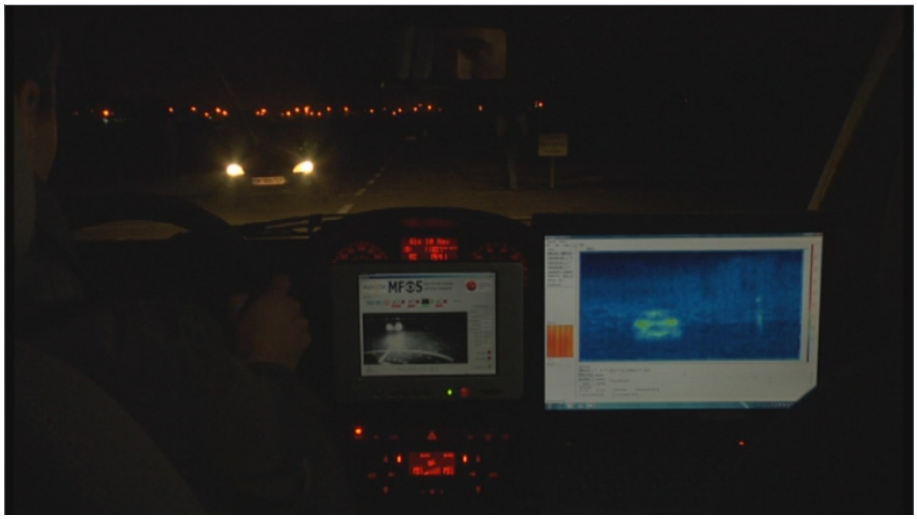

Figure 23 - Warning night vision demo

Two highlights during the demonstration event. On the left side the pre-crash side impact scenario and on the right the warning night vision one.

6. CONCLUSIONS

Twilight and tunnel functions performances have been assessed in many conditions, some of which critical and suitable to stress the function behaviour. Although quantified evaluation and comparison (with SOA sensors) thresholds have not been a-priori defined, the MFOS sensor proved to satisfy common functional requirements that could be verified by trained customers.

The assessment of the fog function have been done in different scenarios and illumination conditions. Although the number of trials seems not to be particularly high, the considered conditions under which the trials have been performed allow to reach some conclusions. Fog function performances in terms of missed detections are affected by vehicle speed, particularly in not-homogeneous fog particle density conditions, and by high environmental illumination levels which limit the functional dynamic range due to the combination of the emitting infrared output of the illuminator and the FOV. In particular the latter limitation could be overcome by adopting dedicated collimating optics. Furthermore, no false positive errors have been observed.

Despite the not fully integration of the rain function in the ADOSE SW framework, a validation and assessment of the functionality performances have been carried out not only in stationary conditions but also in real outdoor scenarios. The selected approach for the detection of the rain droplets is promising and performances could be further improved adopting design strategies aiming at overcoming the identified limitations.

The limited FIR camera specs affected the overall detection performances. By the comparison of the images provided by a commercial FLIR camera rescaled to the resolution of the FIR one it could be figured out that the low resolution (~10°/px horizontal) impacts, as expected, the detection distance. Furthermore, the high thermal noise and the NETD, despite the fact that the tests have been carried out with outside temperature of about 12 °C, degrade the image qualities and the contrast between warm and cold objects. This behavior is also caused by the camera package in its preliminary version. More in details it could be said that the detection is not affected by different car types and the human shape has an high impact (+25%). The maximum detection distances was 60m for a vehicle and 35m for a pedestrian. The low camera frame rate (around 5Hz) did not allowed to detect any obstacle with vehicle speed of more than 20km/h and target vehicle speed of more than 10km/h.
Last trials carried out using the final FIR camera version during the ADOSE final demo session demonstrated the potential benefits of the low cost and low resolution FIR camera technology. Even if not all the target specs have been reached the 100x50 px camera resolution together with the low thermal noise showed the possibility to clearly identify pedestrian obstacles up to 50m distance and hot pixels blobs up to 70m.

The performance achieved with the SRS sensor by the final algorithm gives a standard deviation of the distance of a detectable object of 0.52m in relation to the required 5m critical distance.
With the results achieved by the sensor prototype assessed in real scenario, we conclude that the SRS together with its stereo matching and detection algorithms developed in this project are capable to meet the requirements even with the short baseline of 15 cm (45 cm of the first laboratory prototype).
The intention of the SRS to address the Automotive the Pre-Crash Warning/Preparation Side Impact, the Smart Airbags and the Lane change detection applications is proved to be valid.
In the long term, the SRS with its relatively low cost and fast response time has the potential to add value to the automotive market.

7. LIST OF FIGURES

8. LIST OF TABLES

9. LIST OF ACRONYMS

AC	Alternative Current
AVI	Audio Video Interleave
B&W	Black and White
bks	Backscattering

CAD	Computer Aided Design
CW	Continuous Wave
DC	Direct Current
FIR	Far Infrared
FLIR	Forward looking infrared
FOV	Field Of View
FOV	Field of View
fps	frame per second
GUI	Graphical User Interface
HDR	High Dynamic Range
HFOV	Horizontal Field Of View
Hz	Hertz
IRLED	InfraRed Light Emitting Diode
LIDAR	Light Detection and Ranging
MFOS	MultiFunctional Optical Sensor
MPEG	Moving Picture Experts Group
NETD	Noise-equivalent temperature
NIR	Near Infrared
PCB	Printed Circuit BoardPolyCarbonate
PGM	Portable Gray Map
PMMA	PolyMethylMethAcrylate
ROI	Region Of Interest
SRS	Silicon Retina Sensor
SW	Software
TFT	Thin Film Transistor display
VFOV	Vertical Field Of View
VIS	Visible